Elastic Collisions on a Simulated Circular Air Track

Elastic Collisions on a Simulated Circular Air Track

C. B. Price, *Department of Computing, University of Worcester WR1 3AS, United Kingdom*.
(corresponding author) c.price@worc.ac.uk ORCID 0000 0002 2173 9897

M. L. Pethybridge, *Prince Henry's High School, Evesham, WR11 4QH, United Kingdom*.

Editor's Note: Students in introductory courses often analyze one-dimensional elastic collisions between carts on wheels or gliders on an air track. If the track possesses end stops, and the system is left undisturbed after the initial contact, multiple collisions will occur. The analysis of repeated collisions can be somewhat complicated due to the end-stop reflections. In this article, the authors consider a clever simplification involving a circular track without end-stops. This renders the mathematical analysis more tractable for students, and the system presents a variety of interesting behaviors to explore. Students and instructors will enjoy this entertaining application of linear algebra and can freely make use of online computer simulations provided as supplementary material.

Abstract

Elastic collisions of gliders on linear air tracks are often used to explore conservation of energy and momentum. If one is interested in the glider behavior over a long time span, the analysis involves repeated collisions and is complicated by reflections from the track end-stops. Here we analyze elastic collisions on a novel circular air track; since such a track lacks end-stops, the mathematical analysis of repeated collisions is amenable to our students. Our analysis uncovers a variety of interesting behaviors which depend on the ratio of the glider masses. We examine periodic sequences where the gliders return to their initial conditions and progressions where (when plotted in polar coordinates), the collision positions take on the locus of a spiral. One set of initial conditions produces an 'angle trap' where one glider remains within a certain angular range. We also explore making one glider's mass hypothetically negative which results in a novel 'chasing' motion. Our results were obtained using a 3D interactive simulation (created using C++ within the Unreal engine) which we make available as supplementary material.

I. INTRODUCTION

In high school and college physics classes, linear air tracks are often used in lecture demonstrations or in laboratory exercises[1,2]. A typical configuration is shown in Fig.1(a) where two gliders (equipped with elastic or magnetic bumpers) can collide with each other and with end stops. Experiments usually focus on a single glider-glider collision to demonstrate momentum (and sometimes energy) conservation. If the gliders are left untouched following this initial collision, they rebound from the end stops and then experience further glider-glider and glider-end stop collisions.

The ensuing motion is complex, yet anyone who has performed this experiment may have noted something quite magical: if one glider starts at rest, then at some time in the future (after multiple collisions), it will come to rest again. This complex situation has already been analyzed; a matrix description[3] explains many observed regularities. Despite its elegance, such an analysis may be beyond what is expected of most students, so we propose a simplified arrangement.

In this paper, we present a novel approach which avoids complexities resulting from the end stops; we theoretically analyze elastic collisions on a circular air track where gliders can only collide with each other, Fig.1(b). We are not aware of any existing complete experimental apparatus, though a promising partial apparatus exists: the circular magnetic levitation track[4] using high-temperature superconductors. Due to the absence of a physical device, we created a computer simulation to investigate phenomena that a future experimental setup may exhibit. Our simulation framework, written in C++, numerically solves the differential equations of motion of two interacting gliders using a standard adaptive time-step approach[5]. The framework makes use of the Unreal video game engine[6] for an enhanced user experience, and for 3D visualization. Our simulator is provided as supplementary material; we also include user instructions, some guided and open-ended investigations[7], as well as details of the underlying mathematics.

It is important to understand our use of the simulation framework in the context of this paper, which focuses on analytical results. Our initial simulation investigations, which serve as a substitute for physical experimentation, led to some novel observations; this prompted the theoretical analysis presented in Sections II, III and IV. Figs. 3,5 and 6 are outputs of the simulation framework. The parameters of our model are the mass ratio $\mu = m_2/m_1$ and the gliders' pre-collision velocities v_1 and v_2. For simplicity, we investigated situations with $v_2 = 0$. Our observations were as follows:

1. Following the initial collision, m_2 returned to rest after each even-numbered collision.
2. The speeds of m_1 and m_2 after each odd-numbered collision depended on the value of μ.
3. For specific values of μ, m_2 was found to be at rest at its initial location on the air-track after a certain number of collisions. For example, with $\mu = 3$, after 4 collisions and 1 complete revolution around the track, the gliders returned to their initial locations and initial velocities.

The first result, although not observable on a linear air-track, is expected by the conservation of momentum, where the glider velocity difference is reversed after each collision. The second result makes intuitive sense based on experience working with a linear air-track. We found the third point surprising and intriguing, and it was this novel observation that led to the present analysis, and resulted in an investigation of the conditions necessary to produce this behavior.

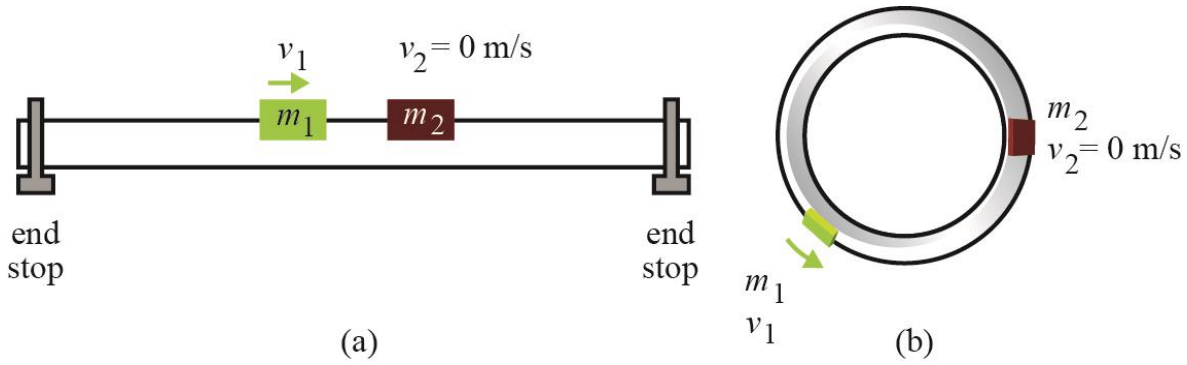

Fig. 1. (a) The linear air track is shown. The end stops reverse the gliders' velocity upon contact. (b) A schematic of a continuous circular air track without end stops.

II. THEORETICAL MODEL

In this section, we develop a theoretical model for elastic collisions on a circular air track. It is convenient to represent the linear velocities of the masses as a vector. It is straightforward to write the textbook[1] result relating the velocities following the i-th and the (i+1)th collisions as a matrix equation

$$\begin{bmatrix} v_1 \\ v_2 \end{bmatrix}^{(i+1)} = \boldsymbol{A} \begin{bmatrix} v_1 \\ v_2 \end{bmatrix}^{(i)}, \tag{1}$$

where the matrix $\boldsymbol{A}$ is

$$\boldsymbol{A} = \frac{1}{1+\mu}\begin{bmatrix} (1-\mu) & 2\mu \\ 2 & -(1-\mu) \end{bmatrix}. \tag{2}$$

This matrix has interesting properties; for example, its square is the identity matrix

$$\boldsymbol{A}^2 = \boldsymbol{I}, \tag{3}$$

so that after two collisions, the gliders recover their original velocities. This means that the gliders will always show a 'period-2' behavior, where they alternate between velocities $[v_1, v_2]$ and $\boldsymbol{A}\,[v_1, v_2]$. Of course, this periodicity is an essential property of elastic collisions.

The time T between subsequent collisions is constant. This important result follows from momentum and kinetic energy conservation. Imagine sitting on mass 2, then we see mass 1 moving with velocity $v_1 - v_2$ the magnitude of which is invariant in one-dimensional elastic collisions. If we assume the circular track has radius R, the time interval between all successive collisions is therefore given by

$$T = \frac{2\pi R}{|v_1 - v_2|}. \tag{4}$$

In what follows, we assume m_2 starts at rest (Fig. 2a), and we further assume $\mu > 1$ so the lighter mass is the one which is initially moving. Under these conditions, the masses move in opposite directions after the first collision (Fig. 2b). Finally, m_2 returns to rest after the second collision (Fig. 2c). This sequence then repeats, which is a great simplification over the linear air track

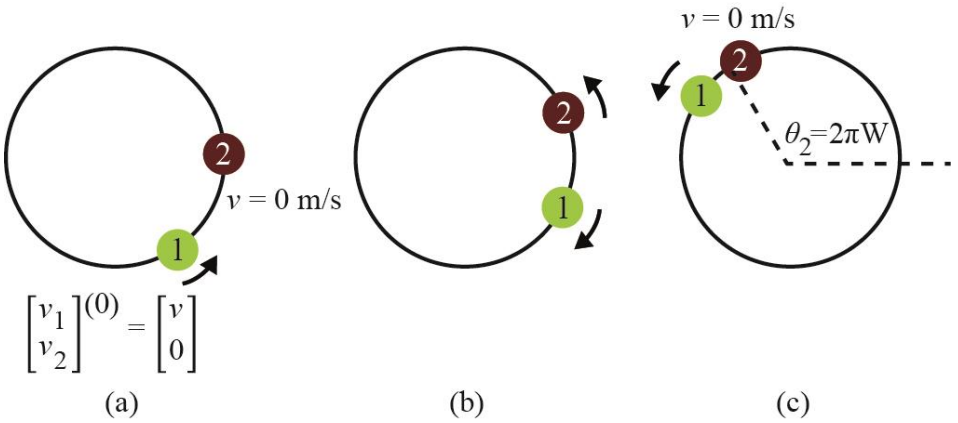

Fig. 2. Collision stages when the lighter, initially moving mass 1 collides with a heavier, initially stationary mass 2: (a) Mass 1 approaches mass 2. (b) Mass 1 reverses direction, mass 2 is propelled forward after the collision. (c) Following the second collision mass 2 is at rest, and its angular displacement is indicated.

behavior. For simplicity, we denote m_1's initial speed as v, then from Eq. (2) we have the following expressions for subsequent velocities

$$\begin{bmatrix} v_1 \\ v_2 \end{bmatrix}^{(2i)} = \begin{bmatrix} v \\ 0 \end{bmatrix} \qquad \begin{bmatrix} v_1 \\ v_2 \end{bmatrix}^{(2i+1)} = \frac{1}{1+\mu} \begin{bmatrix} (1-\mu) \\ 2 \end{bmatrix} v. \tag{5}$$

From Eq. (5) it can be deduced that, for $\mu < 3$, mass 2 emerges with a larger speed than mass 1. For $\mu = 3$ both masses emerge with the same speed, and for $\mu > 3$ mass 1 emerges with a larger speed. Theoretical results derived for this special case may be generalized to the situation of $v_2 \neq 0$ by a simple change of reference frame.

III. RETURN TO THE INITIAL CONDITIONS

In our simulations, we observed behavior which surprised and intrigued us: for certain values of μ, the gliders returned to their initial conditions (often after multiple collisions and several revolutions around the air track). In this section, we obtain expressions for those values μ which lead to this

behavior, the angles covered between collisions, and the number of collisions and revolutions around the air track before the initial state is recovered.

First, from Fig.2 (c) we have

$$\theta_2^{(2)} = \theta_2^{(1)} + 2\pi W \tag{6}$$

where W is the winding number-the fraction of the circle traversed by m_2 prior to the second collision. Since m_2 travels with velocity $v_2^{(1)}$ following its first collision, it traverses an angle $\Delta\theta_2 = v_2^{(1)}T/R$ until its second collision. Using Eq. (4) in the special case of $v_1 = v$ and $v_2 = 0$, we have $T/R = 2\,\pi/v$ and so, when it is moving, mass 2 will always cover an angle between collisions

$$\Delta\theta_2 = 2\pi W = 2\pi\left(\frac{2}{1+\mu}\right). \tag{7}$$

Assuming $\theta_2 = 0$, initially, and repeating this *n* times, we find the angular position of m_2 after $2n$ collisions ($n = 1,2,3\ldots$) is

$$\theta_2^{(2n)} = 2\pi W n. \tag{8}$$

According to (8), mass 2 will be found at rest at its original position after $2n$ collisions if the combination Wn is an integer. Let us assume W is rational so we can write $W = p/q$, (where p and q are positive integers) as a fraction in its lowest terms. Then, the first time Wn equals an integer is when $n = q$ (after $2q$ collisions). At this point in time, we have

$$\theta_2^{(2q)} = 2\pi\frac{pq}{q} = 2\pi p, \tag{9}$$

which tells us that m_2 has made p revolutions around the track. The key result is that the masses will return to their original configuration when W is rational and the mass ratio μ satisfies

$$\frac{p}{q} = \left(\frac{2}{1+\mu}\right). \tag{10}$$

Some examples showing the number of collisions and revolutions prior to recovery of the initial conditions are given in Table 1. Note that μ does not necessarily need to be a whole number for this to occur. Additional values of μ which lead to a recovery of the initial conditions are given in Appendix A.

μ	1	5/3	2	3	5	7
$\frac{p}{q} = \left(\frac{2}{1+\mu}\right)$	1/1	3/4	2/3	1/2	1/3	1/4
$\Delta\theta_2$	360^o	270^o	240^o	180^o	120^o	90^o
$N_C\ (=2q)$	2	8	6	4	6	8
$N_R\ (=p)$	1	3	2	1	1	1
v_1/v	0	-1/4	-1/3	-1/2	-2/3	-3/4
v_2/v	1	3/4	2/3	1/2	1/3	1/4

Table 1. Examples of collision behavior for various values of μ which cause the masses to eventually recover their initial conditions. N_C is the total number of collisions before mass 2 is found at rest at its original position, and N_R is the number of revolutions before this occurs. We also give the velocities of the masses when they emerge from odd-numbered collisions as a fraction of m_1's initial velocity.

Our simulation framework can be used to help visualize such collision sequences. Some example plots are shown in Fig. 3. The Octave scripts used to draw the plots are automatically generated by the simulation framework.

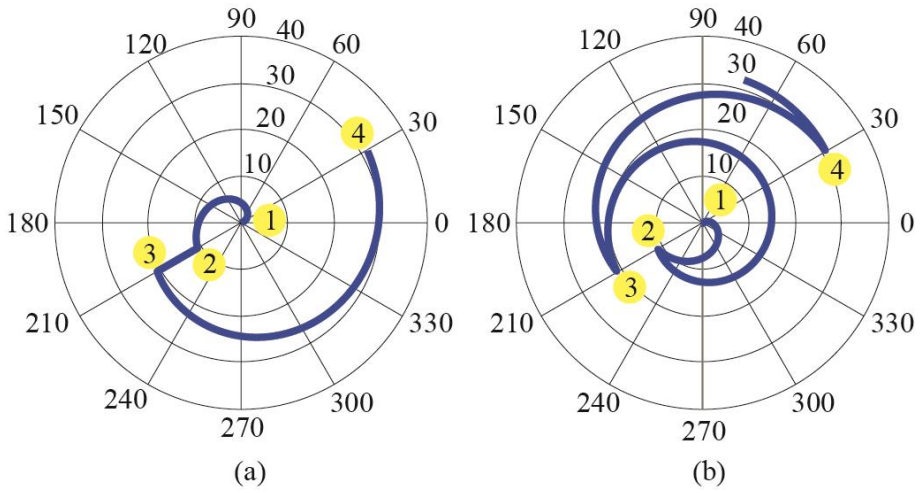

Fig. 3. Polar plots showing glider trajectories, where the angle is shown in degrees, and time (plot radius in seconds) is increasing radially outwards. This example was made with $\mu = 3$; other parameters were chosen so that the time between collisions was approximately 1.0s, and we set $\theta_2^{(0)} = 30^o$ to make the visualizations clearer. The first four collisions are labelled. (a) The trajectory of m_2 showing that it returns to rest at its original location after 4 collisions. (b) The corresponding mass-1 trajectory.

IV. ADDITIONAL NOVEL BEHAVIOR

Having explained the intriguing 'recovery of initial conditions' phenomenon, we now examine whether our theoretical model can predict other interesting behaviors, some of which we observed in our simulations.

A. Angular Traps

The two eigenvalues of matrix $\boldsymbol{A}$ are $+1$ and -1. The negative eigenvalue with associated eigenvector

$$\begin{bmatrix} v_1 \\ v_2 \end{bmatrix} = \begin{bmatrix} -\mu \\ 1 \end{bmatrix} \tag{11}$$

suggests an interesting special case[i], where we find that

$$\boldsymbol{A}\begin{bmatrix} -\mu \\ 1 \end{bmatrix} = \begin{bmatrix} \mu \\ -1 \end{bmatrix} \tag{12}$$

so that the velocities are reversed (not interchanged) on each collision. It is straightforward to calculate the angles of collision, the situation is shown in Fig. 4.

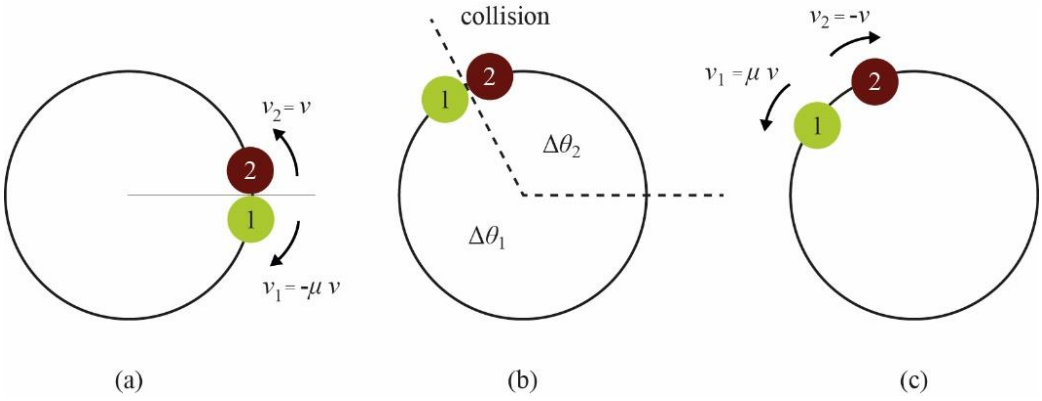

Fig. 4. An example collision for the special case of Sec. IV-A where the velocities are reversed upon collision. (a) Initial conditions. (b) Location at the subsequent collision. (c) Following the collision, the velocities are reversed.

[i] The positive eigenvalue corresponds to the trivial situation; its associated eigenvector indicates that both masses have the same velocity and hence no collision occurs.

Consider an example where mass-2 has initial velocity $v_2 = v$ and mass-1 has initial velocity $v_1 = -\mu v$ and assume that the collision happens after mass-2 has moved through an angle $\Delta\theta_2$. Substituting these values into Eq. (4) gives the time between successive collisions

$$T = \frac{2\pi R}{v(1+\mu)} \tag{13}$$

and therefore, since here $v_2 = v$

$$\Delta\theta_2 = \frac{2\pi}{1+\mu}. \tag{14}$$

After the collision, $v_2 = -v$ so $\Delta\theta_2$ is inverted and m_2 returns to its original position. Mass 2 oscillates between its original position and $\Delta\theta_2$ given by the above expression. Eqs. (13) and (14) show that the period of the collisions and the angular displacement of m_2, are both inversely proportional to $1+\mu$. These examples suggest an 'angle trap' where the faster moving m_1 constrains m_2 to remain within a certain angular range. Eq. (14) can be used to calculate μ for a desired trap angle. Fig.5 shows the trajectory of m_2 in two such simulation examples.

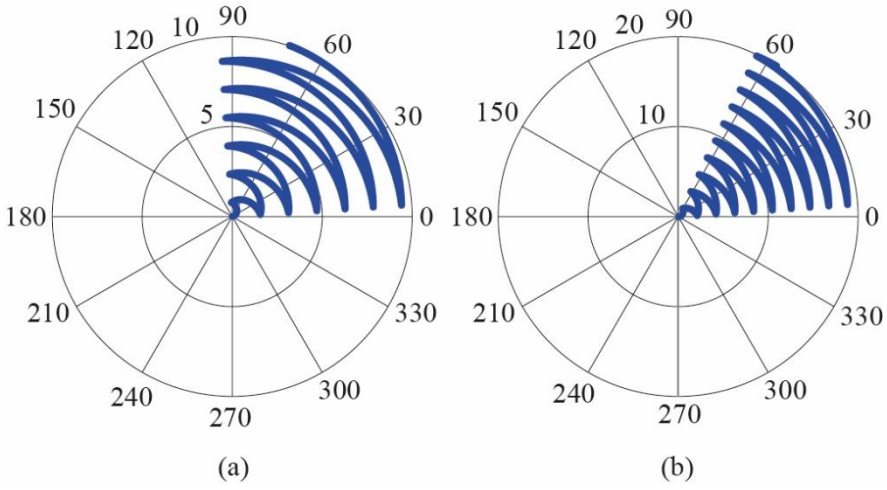

Fig. 5. Simulated trajectories of m_2 where the initial velocities are $v_1 = -\mu$ m/s and $v_2 = 1$ m/s. Angles are in degrees and time (curve radius) in seconds. Note that we introduced an initial offset between the masses to avoid a computational singularity. (a) The case with $\mu = 3$ constrains m_2 to the range $0 \leq \theta \leq \pi/2$. (b) The case of $\mu = 5$ constrains m_2 to the range $0 \leq \theta \leq \pi/3$.

B. The case of 'long' trajectories

The examples shown in Table 1 and Fig. 3 describe 'short' trajectories where return to the initial conditions occurs after a relatively small number of collisions and revolutions. Now we consider 'long' trajectories which evolve through a much larger number of collisions and revolutions before returning

to the initial conditions. To understand these let's start with μ for a 'short' trajectory, e.g, $\mu = 5$, and increase it by a small amount to 5.1. The resulting trajectory will have $p/q = 20/61$ which corresponds to 61 pairs of collisions over 20 revolutions, a 'long' trajectory. Thus, a 'long' trajectory can be obtained through a slight perturbation of a 'short trajectory' mass ratio.

We can explore this mathematically as follows. The winding number for our original 'short trajectory' expression (with $\mu = 5.0$) is

$$W = \left(\frac{2}{1+\mu}\right). \tag{15}$$

A 'long trajectory' can be found by introducing a slightly different mass ratio $\mu' = \mu + \alpha$ where α is a small nudge to μ, (here $\alpha = 0.1$),

$$W' = \left(\frac{2}{1+\mu'}\right) = \left(\frac{2}{1+\mu+\alpha}\right) = \left(\frac{2}{1+\mu}\right)\left(1+\frac{\alpha}{1+\mu}\right)^{-1}. \tag{16}$$

Assuming that $\alpha \ll (1+\mu)$, expanding the rightmost term as a series, and ignoring higher powers, we find the difference in winding numbers is

$$W - W' = \frac{2\alpha}{(1+\mu)^2}. \tag{17}$$

Now that's interesting, since it's proportional to α which defines a constant retard (or advance) of the collision angle relative to the angle of the original with $\mu = 5.0$. This advance or retard will occur for all subsequent collisions as shown in Fig. 6.

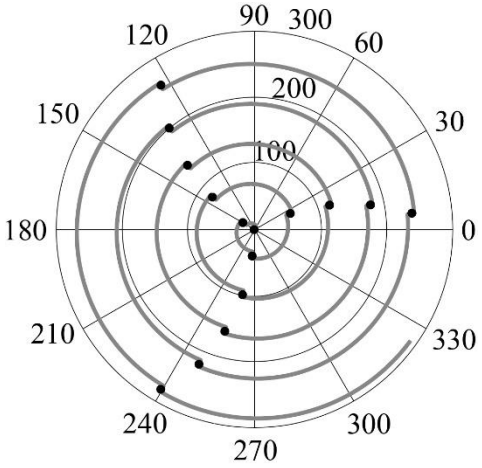

Fig. 6. Simulated trajectory of m_2 for $\mu = 5.1$ overlain with points indicating the theoretical rest angles from Eq. (B3). Angles are in degrees and time (curve radius) in seconds. A similar plot made with $\mu = 5.0$ would show three radial lines of points separated by $120°$ from each other.

The ‘long trajectories’ provide an opportunity to plot the motion over many collisions and revolutions. Such plots (like the one in Fig. 6) suggest that the loci of positions where m_2 returns to rest form a spiral. As shown in Appendix B, this is indeed an Archimedean spiral, where the radius of each point on the spiral is proportional to its angle. The Archimedean spiral is evident when the ‘long trajectory’ data is plotted as in Fig. 6, but it is in fact a general feature of all trajectories (short, or long). In Appendix B, we show that the loci of positions where m_2 returns to rest lie on an Archimedean spiral regardless of the mass ratio.

C. The Case of Negative Mass

Hypothetical situations challenge our students’ conceptual understanding and provide learning opportunities. One such situation involves hypothetically allowing m_2 to be negative and exploring the consequences. It may seem at first strange to entertain the concept of negative mass, but there are precedents e.g., in semiconductor band theory where electrons can have negative mass[8,9]. Negative mass forms a part of the ‘dynamic-equivalence approach’ to gravitational systems[10] and can be engineered in quantum systems[11].

The analysis of hypothetical situations involving negative mass can be surprising and interesting. Simulations where m_2 is negative follow the pattern shown in Fig. 7. Following the collision between a moving m_1 and a stationary m_2, both gliders emerge with a negative velocity, with m_1 moving faster than m_2. This is because during the collision, both masses experience forces in opposite direction of their approach velocities, but since $m_2 < 0$, it accelerates in the *opposite* direction to the force experienced. This behavior can be understood analytically as follows.

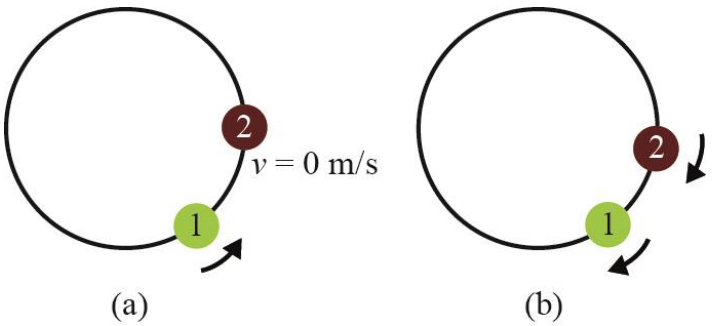

Fig. 7. (a) The moving mass 1 approaches a stationary mass 2 whose mass is negative. (b) Following the collision, both masses move in the same direction. This behavior can be compared with the positive mass situation shown in Fig. 2.

Consider the situation where $\mu < 0$, in this case we have $\mu = -|\mu|$. The square of the matrix $\boldsymbol{A}$ is the identity matrix (regardless of the sign of μ), so period-2 collisions in time will still be obtained. The expressions for the velocities after a collision with a stationary m_2 are

$$\begin{bmatrix} v_1 \\ v_2 \end{bmatrix}^{(2i+1)} = -\frac{1}{|\mu| - 1} \begin{bmatrix} (1 + |\mu|) \\ 2 \end{bmatrix} v. \tag{18}$$

Unlike in Eq. (5), we see that here both masses move in the same direction. If the masses are to separate, then following the collision we must have $|v_1| > |v_2|$ which from Eq. (18) implies that $|\mu| > 1$, and both velocities are negative (we define m_1 to have positive velocity before the collision): Mass 1 'chases' mass 2. Since both masses are moving in the same direction, they can cover a larger angular distance than if $m_2 > 0$, e.g., for $\mu = -2$, m_2 covers 720^{o} before it returns to rest.

For $|\mu| > 3$ both gliders are moving faster than glider 1 on its approach, which at first sight seems to violate conservation of energy. However, the analysis of energy must be treated with care; since $m_2 < 0$, its kinetic energy is actually negative.[ii]

Negative mass has been discussed in the context of the gravitational force before[12], but we hope that inserting a negative mass into an elastic collision provides readers an opportunity to engage with this non-intuitive and challenging concept.

V. CONCLUSIONS

Compared with a linear air track, a circular air track simplifies the kinematics of multiple glider collisions by avoiding complications associated with end-stop reflections. We have shown that this system presents a rich variety of behavior. Using matrix algebra, we have presented some closed-form solutions, which could be valuable in high-school or college classrooms and laboratories.

The code and assets for our Unreal engine simulation are freely available as supplementary material[7]. Ultimately, to perform actual laboratory experiments, physical circular air tracks, or some equivalent apparatus, must be developed. We hope that material presented in this paper will inspire

[ii] As an example, consider the situation for $\mu = -2$ and, as usual m_2 is initially at rest. Following the first collision, the gliders emerge with velocities $v_1 = -3v$ and $v_2 = -2v$. It is straightforward to verify that both momentum and energy are conserved by substitution in expressions for momentum and energy before and after the collision.

researchers and equipment manufacturers to develop such a laboratory kit. In the meantime, we hope that our computer simulations will be valuable to educators.

SUPPLEMENTARY MATERIAL

Please click on this link to access the supplementary material, which includes our simulation code along with user instructions. Print readers can see the supplementary material at [DOI to be inserted by AIPP].

ACKNOWLEDGEMENTS

The authors would like to thank Will Osborne for some insightful discussions and Andrew Robinson for production graphics. We would also thank the two expert reviewers whose detailed comments have led to substantial improvements of the initial manuscript.

APPENDIX A: SOME VALUES OF μ RESULTING IN RATIONAL W

p \ **q**	1	2	3	4	5	6	7	8	9	10	11
1		3	5	7	9	11	13	15	17	19	21
2			2	3	4	5	6	7	8	9	10
3				5/3	7/3		11/3	13/3		17/3	19/3
4					3/2		5/2		7/2		9/2
5						7/5	9/5	11/5	13/5		17/5
6							4/3				8/3
7								9/7	11/7	13/7	15/7
8									5/4		7/4
9										11/9	13/9
10											6/5

APPENDIX B: PROOF OF THE ARCHIMEDEAN SPIRAL

Consider a general mass ratio μ and start with m_2 at rest

$$\begin{bmatrix} v_1 \\ v_2 \end{bmatrix} = \begin{bmatrix} v \\ 0 \end{bmatrix}. \qquad (B1)$$

Recall that m_2 does not travel at a constant velocity. As shown in Eq. (5), it actually alternates between speeds of 0 and $2v/(1+\mu)$. As argued in the text, the time interval between collisions is constant, so the mass spends exactly half of its time at rest and half of its time moving.

Therefore, during a full two-collision time interval, m_2 travels with an average angular velocity

$$\omega_{avg} = \frac{v}{R(1+\mu)}\,, \tag{B2}$$

which (because it is only moving half of the time) is half of its angular speed when it is moving. Immediately after each even numbered collision, its angular position would be identical to an object traveling with a constant angular velocity ω_{avg}. Such an object would have an angular position as a function of time

$$\theta(t) = \omega_{avg} t = \frac{v}{R(1+\mu)} t. \tag{B3}$$

Inverting this relationship, we have

$$t(\theta) = \left(\frac{R(1+\mu)}{v}\right)\theta. \tag{B4}$$

A polar plot of this equation (with the radius of the plot being the time t) is an Archimedian spiral. Thus, even though the polar plot of the exact trajectory of m_2 is somewhat complicated (see Fig. 6 for an example) the angular positions of the mass m_2 after $2n$ collisions lie on an Archimedian spiral.

AUTHOR DECLARATIONS

Conflict of Interest

We declare that we do not have any conflict of interest.

[1] A. Tipler and G. Mosca, *Physics for Scientists and Engineers,* (W.H.Freeman and Co., New York, 2008).

[2] H.D. Young and R.A. Freedman, *Sears and Zemansky's University Physics,* (Addison-Wesley, San Fransisco, CA, 2012).

[3] R.H. Romer, "Matrix Description of Collisions on an Air Track," Am. J. Phys. **35**(9), 862-868 (1967).

[4] An example of a circular magnetic levitation kit can be found in the catalogue of the supplier PASCO at this link https://www.pasco.com/products/lab-apparatus/atomic-and-nuclear/se-7721

[5] W.H. Press, S.A. Teukolsy, W.T. Vetterling, B.F. Flannery, *Numerical Recipes. The Art of Scientific Computing. Third Edition* (Cambridge University Press, Cambridge, U.K., 2007).

[6] The Unreal engine is released by Epic Games, and is mainly used to create video games, but has other applications such as film, TV, architecture and simulation. It is free for educational purposes.

[7] Supplementary material is available online at [link to be inserted by AIPP] which comprises the following: (i) User guide to the simulation framework, (ii) guided investigations for Section 3, (iii) suggestions how to explore angle traps, spiral lo9i, negative mass and the effects of friction, (iv) details of the simulation framework. The computer program requires the Windows operating system.

[8] C. Kittel, *Introduction to Solid State Physics* (John Wiley & Sons Inc, New York, 1971).

[9] K-Q. Lin, C. Ong, S. Bange, P. Junior, B. Peng, J. Ziegler, J.Zipfel, C.Bauml, N. Paradiso, K. Watanabe, T. Taniguchi, C. Strunk, B. Monserrat, J. Fabian, A. Chernikov, D. Qiu, S. Louie, and J. Lupton, "Narrow-band high-lying excitons with negative-mass electrons in monolayer WSe_2 ," Nature Communications https://doi.org/10.1038/s41467-021-25499-2 (2021).

[10] N. K. Spyrou, "Negative mass and repulsive gravity in Newtonian theory, and consequences," IOP Journal of Physics: Conference Series **189** (2009).

[11] M. A. Khamehchi, K. Hossain, M. E. Mossman, Y. Zhang, Th. Busch, M. M. Forbes and P. Engels, "Negative-Mass Hydrodynamics in a Spin-Orbit-Coupled Bose-Einstein Condensate," Physical Review Letters **118** (15), (2017)

[12] R. H. Price "Negative mass can be positively amusing," Am. J. Phys **61** (3), (1993).

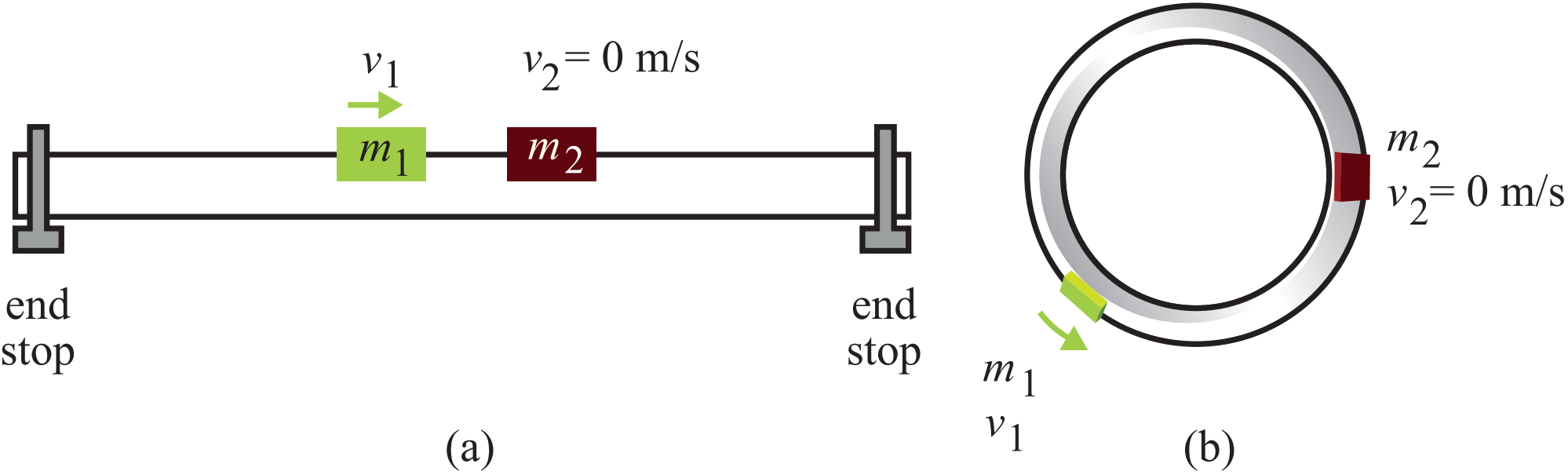
v_1
$v_2 = 0$ m/s
m_1
m_2
end stop
end stop
(a)
m_2
$v_2 = 0$ m/s
m_1
v_1
(b)

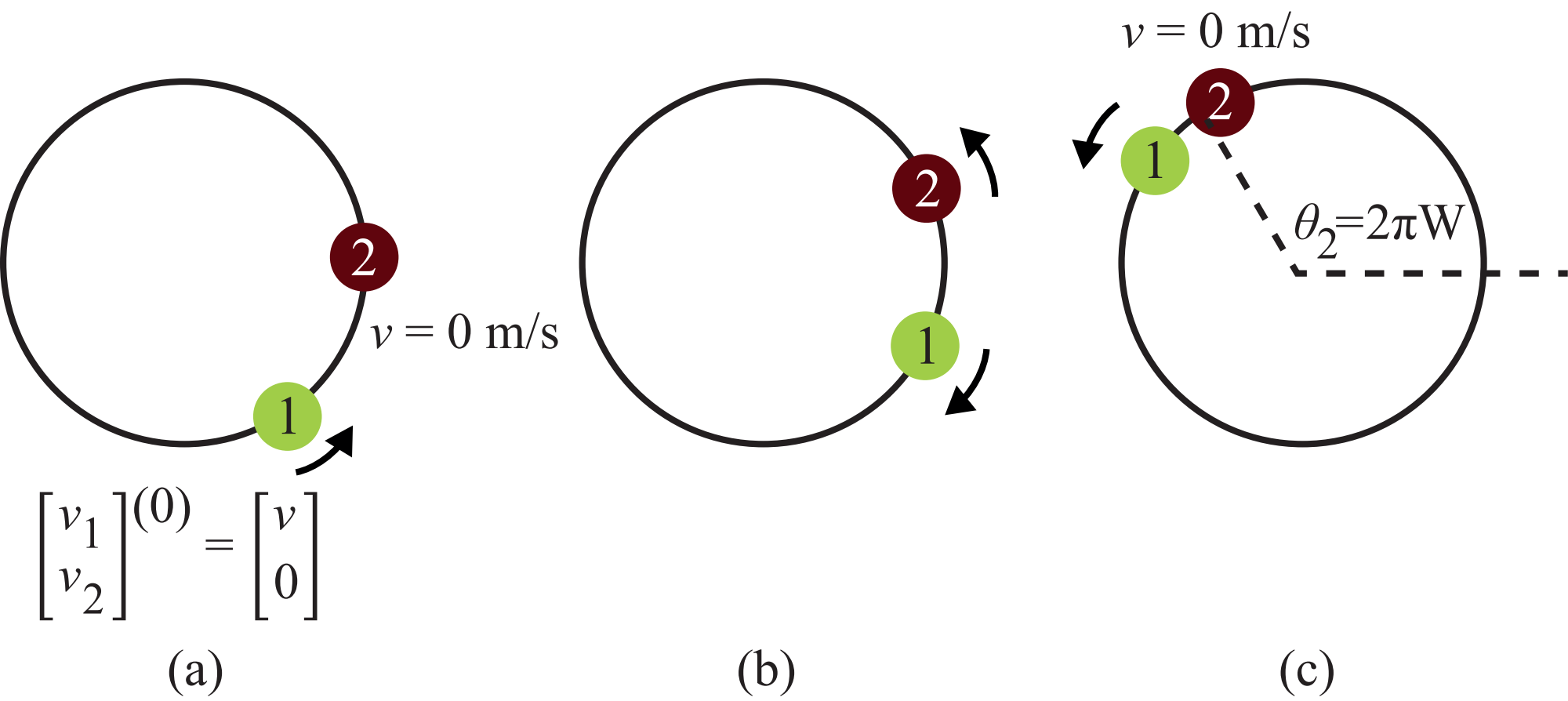
2
1
v = 0 m/s
$\begin{bmatrix} v_1 \\ v_2 \end{bmatrix}^{(0)} = \begin{bmatrix} v \\ 0 \end{bmatrix}$
(a)
2
1
(b)
v = 0 m/s
2
1
θ_2=2πW
(c)

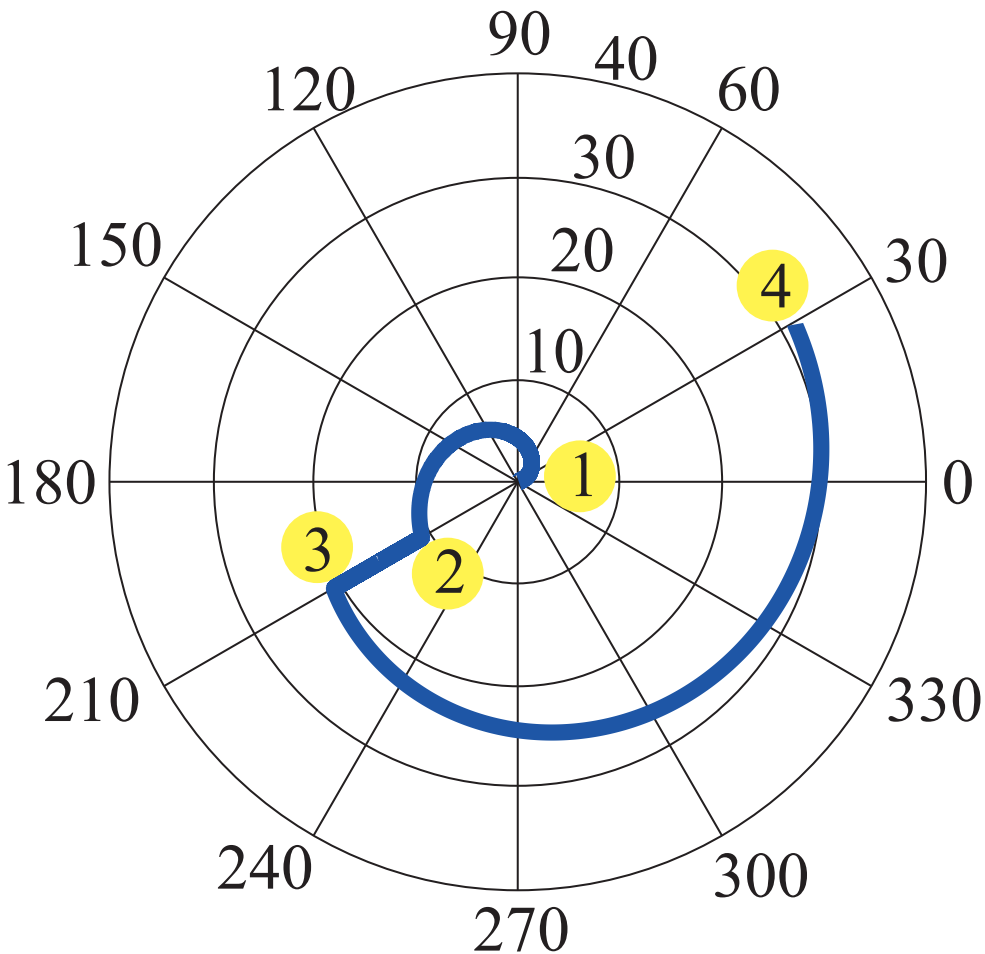
90
40
60
120
30
150
20
30
10
180
0
1
4
3
2
210
330
240
300
270

(a)

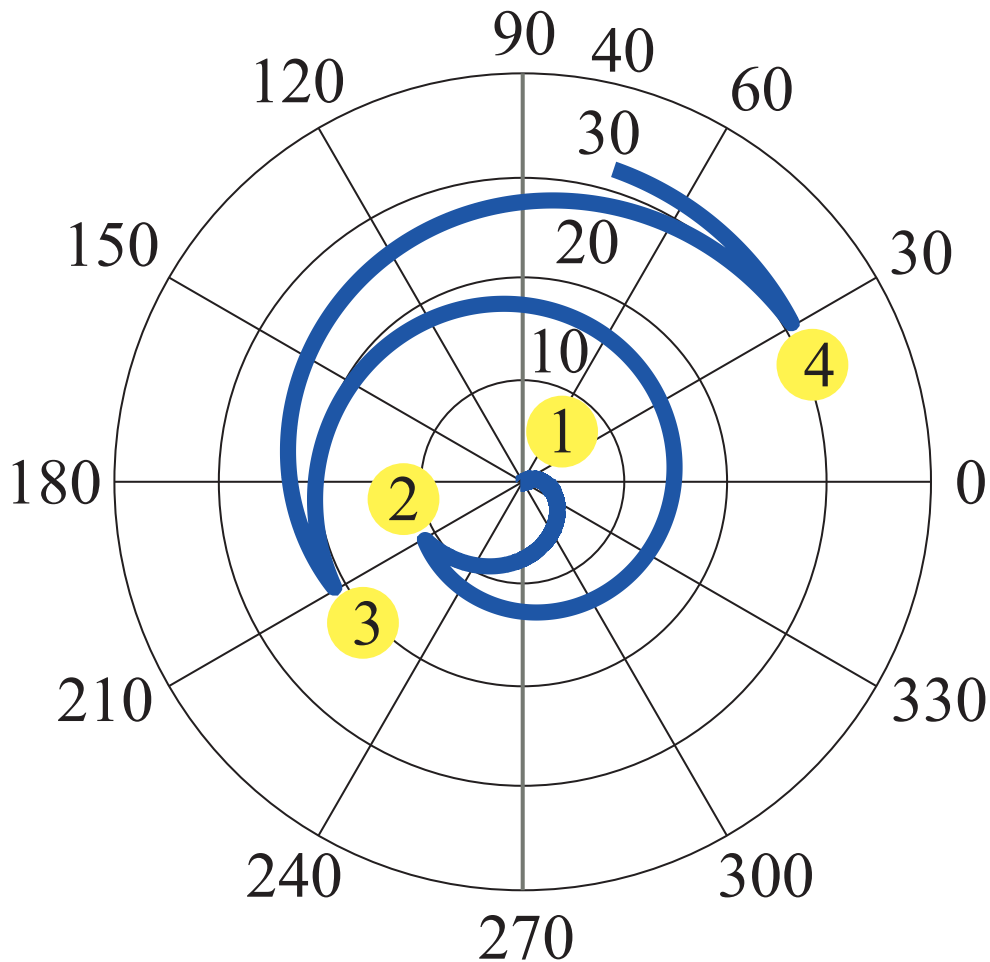
90
40
60
120
30
150
20
30
10
4
1
180
0
2
3
210
330
240
300
270

(b)

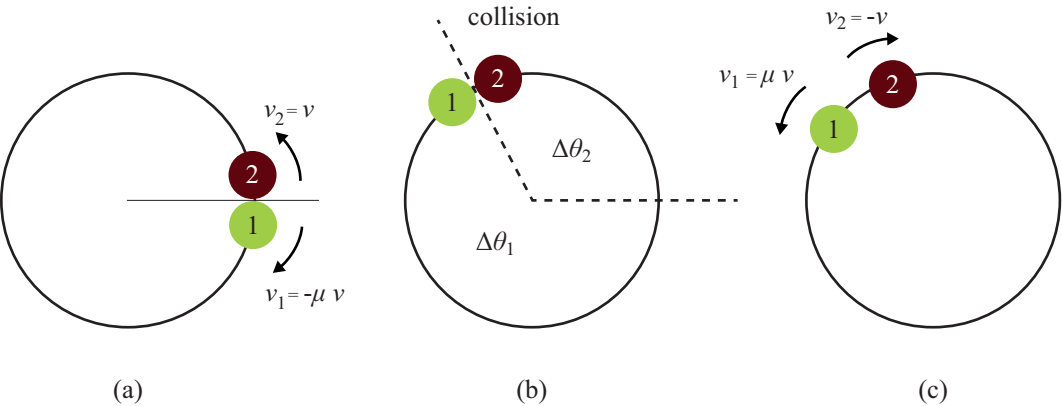
collision
$v_2 = v$
$v_1 = -\mu\ v$
$\Delta\theta_2$
$\Delta\theta_1$
$v_2 = -v$
$v_1 = \mu\ v$
2
1
(a)
(b)
(c)

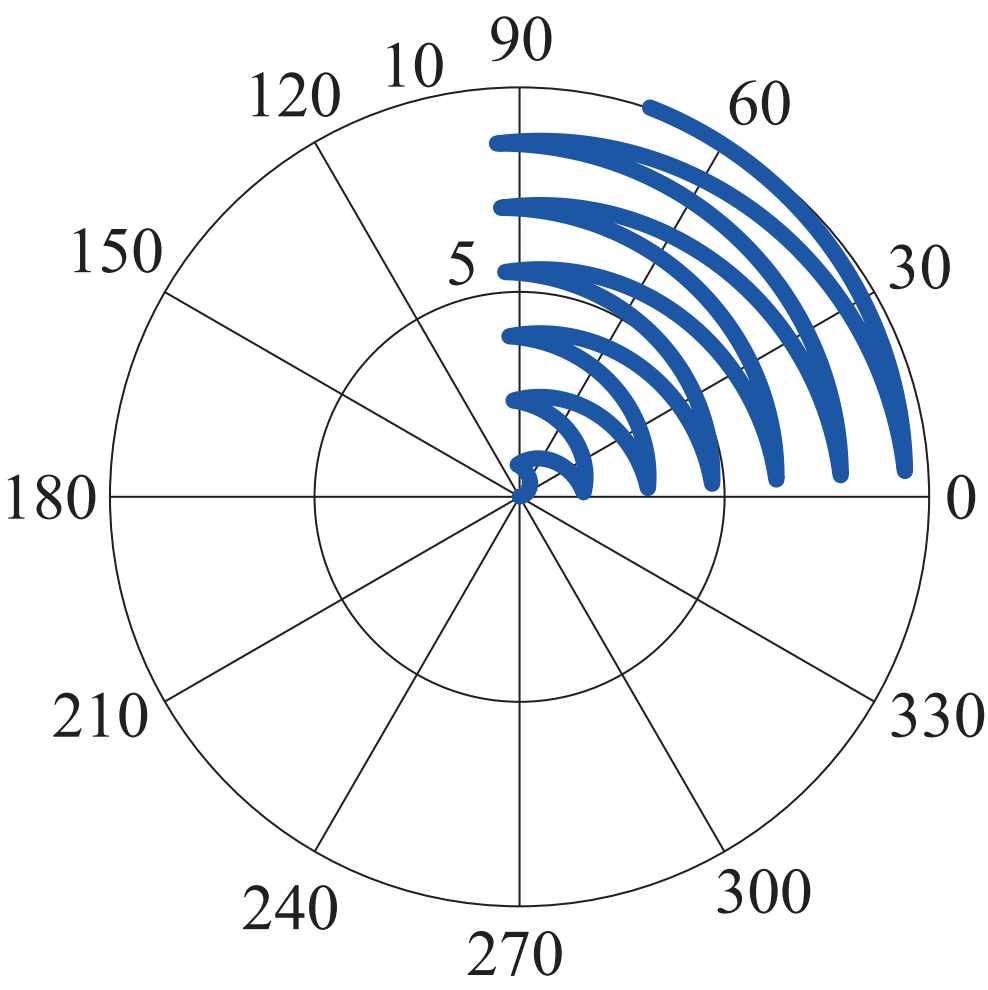
90
10
120
60
150
5
30
180
0
210
330
240
300
270

(a)

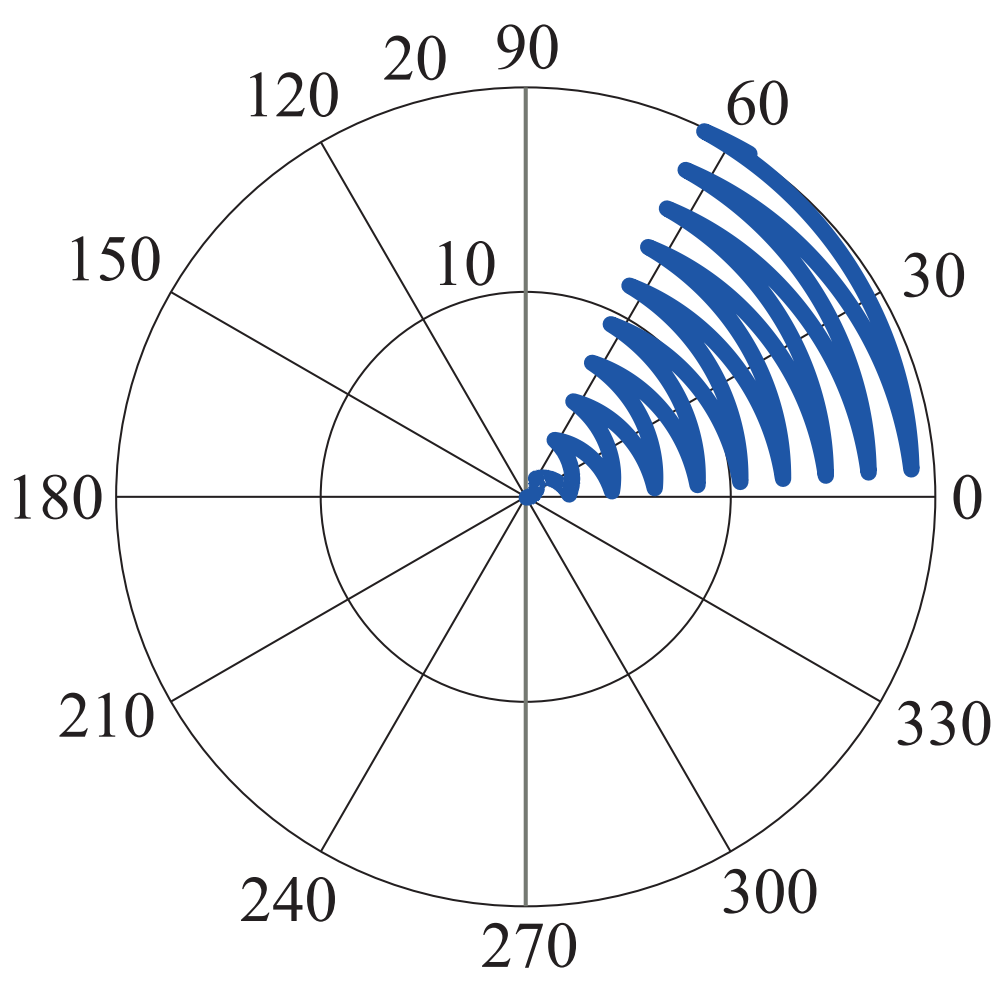
90
20
120
60
150
10
30
180
0
210
330
240
300
270

(b)

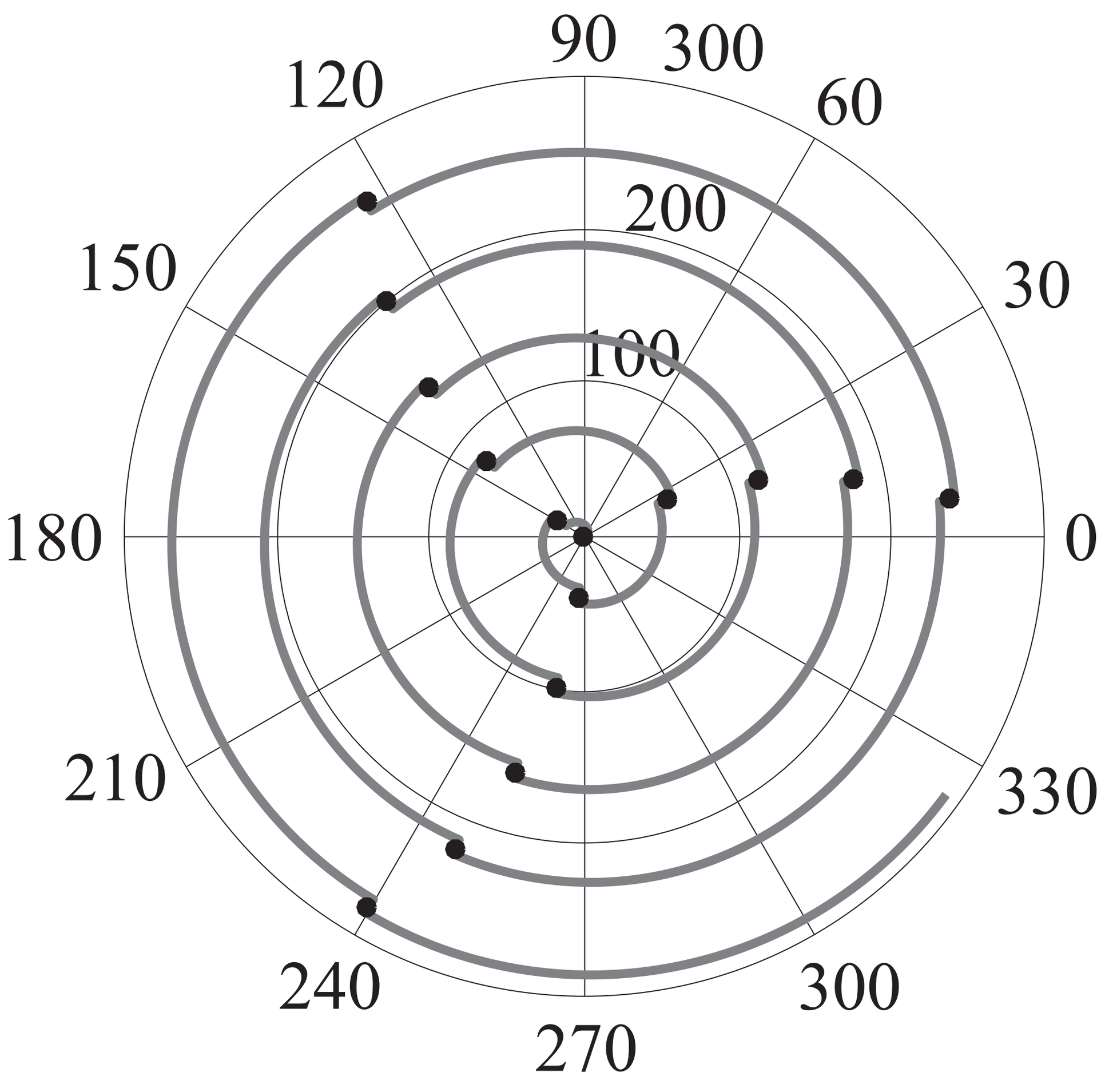
90
300
120
60
200
150
30
100
180
0
210
330
240
300
270

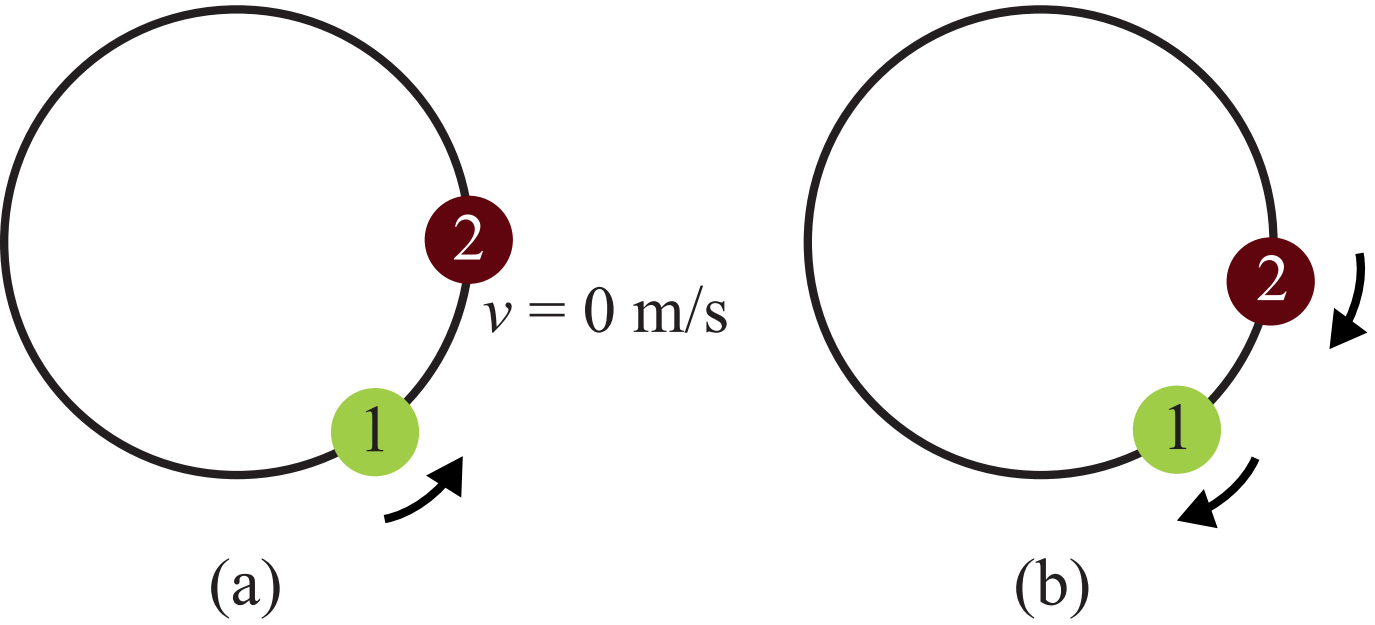
2
$v = 0$ m/s
1
(a)
2
1
(b)